STM JOURNALS

Trends in
Transport Engineering and Applications

ISSN: 2394-7284
Volume 11, Issue 1, 2024
January—April
DOI (Journal): 10.37591/TTEA

https://journals.stmjournals.com/ttea

Research TTEA

Detecting the Failure Stages in Asphalt Concrete Through the Fatigue Life

Saad Issa Sarsam*

Abstract

The signs of failure initiation in asphalt concrete through its service life may appear as cracking, rutting, or other types of distress after practicing dynamic stresses from vehicular loading. This work is concerned with detecting the failure initiation in asphalt concrete in the laboratory, and the role of binder content and constant strain level through a comprehensive testing program. Asphalt concrete mixtures were formulated with the optimal binder content, as well as with binder content adjusted by ±0.5%. These mixtures were then compacted into slab molds using a laboratory roller. From the slab samples, beam specimens were extracted and subjected to fatigue life testing under dynamic flexural stresses in a controlled 20°C environment. The testing program encompassed three constant strain levels: 750, 400, and 250 microstrain. It was observed that the failure occurs in three stages after practicing the dynamic loading. The binder content exhibits a significant influence on the starting point of such stages. However, the impact of constant strain level is more pronounced as the binder content increases. The binder content exhibits a significant influence on extending the fatigue life and controlling the stages of failure.

Keywords: Failure, stages, flexure, asphalt concrete, fatigue, strain level, stiffness

INTRODUCTION

Abojaradeh et al. [1] defined the final and the initial stiffness in the testing for flexure fatigue life of asphalt concrete. Flexure fatigue tests were performed on dense-graded mixtures. Fatigue models were developed using linear regression curve fitting. Test results indicated that the initial stiffness could be obtained after 50 cycles of dynamic loading, while the fatigue stiffness is taken at 50% of the initial stiffness. The obtained stiffness degradation model represents a basic material property. Chen et al. [2] developed a model to represent the relationship between the log of the number of cycles and the log of the stiffness obtained from dynamic bending fatigue test at various strain levels and temperatures. Three transition points were identified which are related with the fatigue progression. It was revealed that the number of loading cycles associated with the first two transition points exhibit no statistically significant differences. The first point is the number of cycles to micro-crack initiation and propagation, while the second point is the true failure point. Bessa et al. [3] assessed hot mix asphalt concrete and the test results were used in different pavement performance models. It was addressed that the conventional mechanistic-empirical pavement design guide overestimates the fatigue life of asphalt pavement since the model does not consider the stiffness of the base layer, the viscoelastic characteristics of the asphalt mixture, and the climate conditions. Abhijith and Narayan [4] stated that the deformation in the asphalt concrete beam specimen is not homogeneous. Such behavior is not given consideration in traditional analyses of test results. Different parts of the asphalt concrete beam specimen would experience different levels of

***Author for Correspondence**
Saad Issa Sarsam
E-mail: saadisasarsam@coeng.uobaghdad.edu.iq

Professor, Sarsam and Associates Consult Bureau (SACB), Baghdad-IRAQ., Formerly at Department of Civil Engineering, College of Engineering, University of Baghdad, Iraq

Received Date: April 26, 2024
Accepted Date: May 02, 2024
Published Date: May 04, 2024

Citation: Saad Issa Sarsam. Detecting the Failure Stages in Asphalt Concrete Through the Fatigue Life. Trends in Transport Engineering and Applications. 2024; 11(1): 21–27p.

damage when subjected to dynamic loading since the strain in the beam varies both along the depth and length of the beam. Based on the study, a new fatigue failure criterion is proposed. The number of repetitions at which the modulus reduces to zero is considered as the point of failure. It was concluded that this fatigue life criterion is more meaningful than the old 50% reduction in stiffness criterion. Mazurek and Iwański [5] compared the test results from the curve fitting of relaxation functions in mechanical and mathematical models with the master curves constructed based on those models. It was revealed that the modeling results will provide an overarching view on the effectiveness of use of each relaxation function. Sarsam [6] assessed the influence of environment and microstrain level on the fatigue life and permanent microstrain of asphalt concrete. It was observed that the permanent microstrain and the fatigue life of asphalt concrete increases at a testing environment of 30℃ as compared with that at testing environment of 5℃. The second model type is the pavement damage model, and the deterioration of pavement can be attributed to the damage related to the decline in pavement serviceability due to accumulation of axle load passes as reported by Pradhan et al. [7].

The aim of the present work is to explore the failure stages of asphalt concrete through the fatigue life when practicing dynamic flexural stresses at 20℃ environment and three levels of constant strain of (750, 400, and 250) microstrain.

MATERIALS AND METHODS

The materials implemented in this work are locally available and usually used for asphalt pavement construction.

Asphalt Cement

The asphalt cement binder, sourced from the AL-Nasiriya Oil Refinery located south of Baghdad, possessed initial physical characteristics including a ductility of 150 cm, a softening point of 49°C, and a penetration grade of 42. Subsequent to subjecting the asphalt cement binder to an accelerated aging process via the thin film oven test, its penetration decreased to 33 cm, while ductility reduced to 83. Conversely, the softening point increased to 53°C. These physical property assessments of the asphalt cement binder adhered to ASTM procedures [8].

Fine and Coarse Aggregates

A blend of natural and crushed fine aggregates, along with crushed coarse aggregates, was sourced from the AL-Ukhaider quarry situated north of Baghdad. Both types of aggregates underwent sieving to achieve various sizes. The bulk specific gravity of the fine and coarse aggregates measured at 2.558 and 2.542, respectively, while their respective water absorption rates were recorded as 1.83% and 1.076%. These assessments of the physical properties of aggregates were carried out in accordance with ASTM procedures [8].

Mineral Filler

The limestone dust was obtained from Karbala quarry, south of Baghdad, and implemented as mineral filler. Testing for physical properties shows that the bulk specific gravity of the mineral filler is 2.617. However, 94 % of the filler passes sieve No. 200 (0.075 mm).

Selection of the Combined Aggregate Gradation for Preparation of Asphalt Concrete Mixture

In the current study, the dense gradation of aggregates typically employed for the wearing course pavement layer was chosen. It follows SCRB [9] specification. The aggregates gradation exhibit 12.5 mm of nominal maximum size of aggregates. Figure 1 demonstrates the implemented aggregates gradation.

Preparation of the Asphalt Concrete Mixture, Slab Samples, and Beam Specimens

The coarse and fine aggregates, along with the mineral filler heated to 160°C, were combined with the asphalt cement binder heated to 150°C. Through the Marshall Test, an optimal asphalt binder content of 4.9% was determined.

Details of the procedure of obtaining the optimum binder requirement can be referred to in the study by Sarsam and Alwan [10]. The prepared asphalt concrete mixtures were compacted in a rectangular slab mold of 300 × 400 mm while the depth of the mold was 60 mm. Laboratory roller compaction was conducted to the target bulk density according to procedure described by EN12697-33 [11]. The details of conducting the compaction process can be referred to Sarsam [12]. The temperature of the compaction was maintained at 150°C throughout the rolling compaction process. After allowing the asphalt concrete slab samples to cool overnight, beam specimens measuring 62 mm in width, 56 mm in height, and 400 mm in length were extracted from the prepared slabs using a diamond saw. A total of three slab samples of asphalt concrete were prepared, while 12 asphalt concrete beam specimens were tested. For the analysis, the average value from testing duplicate beam specimens was taken into account.

Testing for Fatigue by Implementing the Dynamic Flexural Bending Beam Test

The four-point dynamic flexural beam bending test, illustrated in Figure 2, was performed following the test procedure outlined in AASHTO T321 [13]. This test aimed to assess the decline in flexural stiffness of asphalt concrete over its fatigue life, under varying environmental conditions of 5°C and 30°C, along with three consistent strain levels of 250, 400, and 750 microstrain.

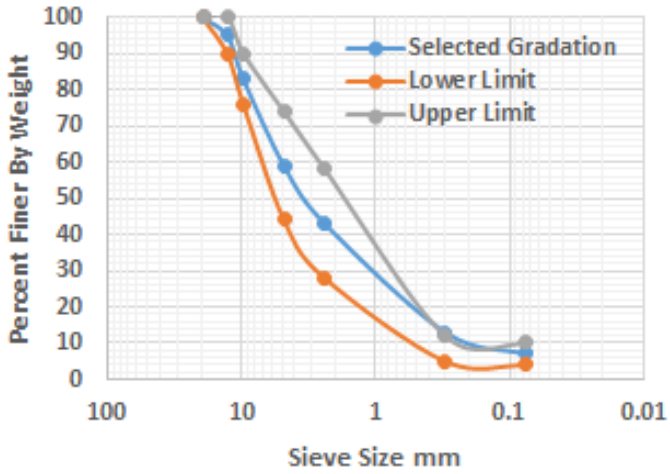

Figure 1. The selected combined aggregates gradation.

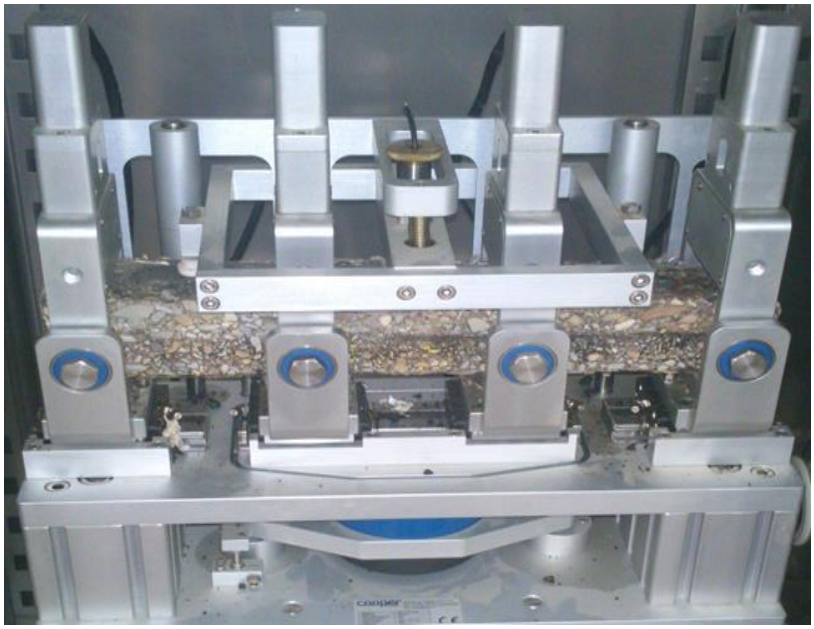

Figure 2. Four-point flexural bending test setup.

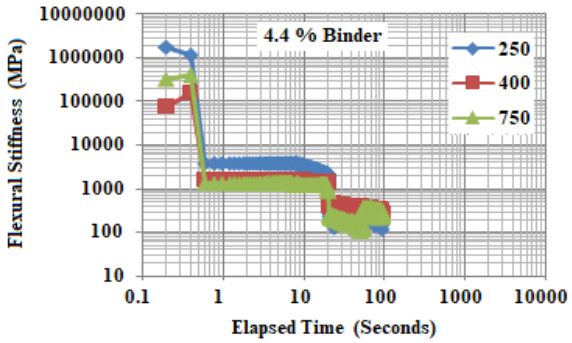

Figure 3. Failure of asphalt concrete prepared with lower binder content.

The beam specimens were stored in the testing chamber for three hours at the specific testing temperature before practicing the dynamic flexural stresses. Similar testing procedure using dynamic stresses, various constant strain levels, and various testing temperatures was adopted by Chen et al. [2].

RESULTS AND DISCUSSION

Failure of Asphalt Concrete Prepared with Lower Binder Content

Figure 3 exhibits the deterioration of the flexural stiffness of asphalt concrete that prepared with 4.4% binder content through the elapsed time since the start of practicing the dynamic flexural stresses. Four stages of failure could be identified, the first stage is just after 0.4 to 0.5 seconds of practicing the flexural stresses. The flexural stiffness starts with a high values, and then declines sharply from 1000000, 300000, and 100000 MPa to 4000, 2000, and 1000 MPa when the applied constant strain is 250, 400, and 750 microstrain, respectively. This stage is associated with possible materials organization and orientation of solid particles of the asphalt concrete mixture which provide a seating effect. In the second stage of failure, the flexural stiffness declines almost linearly at slow rate to 3000, 1500, and 900 MPa when the applied constant strain is 250, 400, and 750 microstrain, respectively, as the loading proceed. In this stage, microcrack formation is expected, and the duration of the second stage is longer than that of the first stage and extended to 20 seconds. The third stage of failure starts after 20 seconds of loading and a sharp drop in the flexural stiffness could be detected. The flexural stiffness declines to 300, 200, and 100 MPa when the applied constant strain is 250, 400, and 750 microstrain, respectively. At the fourth stage of failure, the asphalt concrete beam specimen starts to fracture slowly since the applied flexural stress is reduced with load repetitions and the failure occur after 100 seconds of practicing the dynamic flexural stresses regardless of the implemented constant strain level. The flexural stiffness declines almost linearly to 100, 400, and 500 MPa. It can be revealed that clear definition of the transition between the stages of failure was easy in general since the micro and macro cracking may be tracked or verified during the test due to the stiff and brittle nature of asphalt concrete structure prepared with lower than optimum binder content. Similar behavior was reported by Abojaradeh et al. [1] and Sarsam [14].

Failure of Asphalt Concrete Prepared with Optimum Binder Content

Figure 4 demonstrates the failure mode of asphalt concrete which was prepared with optimum binder requirement of 4.9%. It can be revealed that obtaining a clear definition of the transition between the stages of failure is not easy as in the case of asphalt concrete mixture prepared with lower binder content since the micro and macro cracking cannot be tracked or verified during the test.

The first stage of failure occurs after 0.5 seconds and the flexural stiffness declines from 30000, 90000, and 60000 MPa to 10000, 9000, and 2000 MPa when the applied constant strain is 250, 400, and 750 microstrain, respectively. In the second stage of failure, the flexural stiffness declines almost linearly at slow rate to 7000, 2000, and 1000 MPa when the applied constant strain is 250, 400, and 750 microstrain, respectively, as the loading proceed.

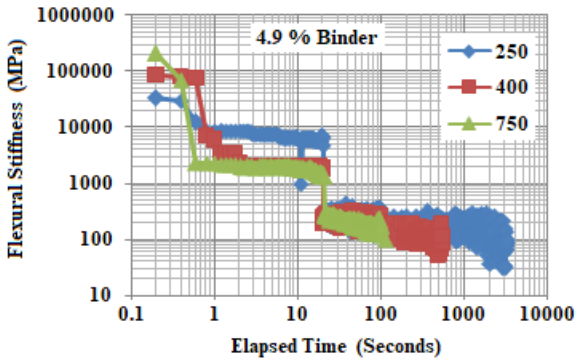

Figure 4. Failure of asphalt concrete prepared with optimum binder content.

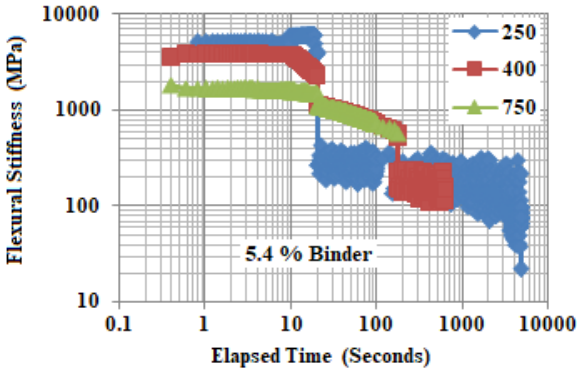

Figure 5. Failure of asphalt concrete prepared with higher binder content.

In this stage, microcrack formation is expected, and the duration of the second stage is longer than that of the first stage and extended to 20 seconds. The third stage of failure starts also after 20 seconds of loading and a sharp drop in the flexural stiffness could be detected. The flexural stiffness declines to 300, 250, and 200 MPa when the applied constant strain is 250, 400, and 750 microstrain, respectively. The fourth and final stage of failure exhibit a gentle and almost linear decline in the flexural stiffness to 30, 100, and 200 MPa and show the longest elapsed time to complete after 4000, 700, and 150 seconds for (250, 400, and 750 microstrain, respectively. Such behavior may be attributed to the dense structure obtained when the optimum binder content was implemented. similar behavior was reported by Abhijith and Narayan [4] and Sarsam [15].

Failure of Asphalt Concrete Prepared with Higher Binder Content

Figure 5 exhibits the failure stages of asphalt concrete prepared with 5.4% binder content, which is higher than the optimum requirements by 0.5%. The starting stage of failure is completely different as compared with the previous mixtures. The first stage of failure shows an almost linear trend up to 20 seconds of practicing the dynamic flexural stresses and the stiffness decline to 4000, 2000, and 1000 MPa for 250, 400, and 750 microstrain levels, respectively. The second stage of failure exhibits sharp drop in the flexural stiffness of asphalt concrete specimen to 500 MPa when a constant strain level of 250 microstrain is implemented. However, more gentle decline of the stiffness to 1000 and 900 MPa could be detected when a constant strain levels of 400 and 750 microstrain was implemented.

The third stage of failure exhibits a gentle drop in the stiffness up to 170 seconds, and the stiffness decline to 300, 400, and 500 MPa. The fourth stage of failure starts after 170 seconds and exhibit almost a linear trend to 100 MPa for 250 microstrain level and a drop to 200 MPa for 400 microstrain level, while the 750 microstrain level shows complete failure after 170 seconds of loading. Such behavior may be related to the possible creep of the asphalt concrete mixture prepared with such high percentage of asphalt binder. It can be revealed that the high binder content has extended the fatigue life of asphalt concrete to 25% and 16.6% for 250 and 400 microstrain levels, respectively, as compared with the mixtures prepared with optimum binder content. On the other hand, the fatigue life of asphalt concrete declined by 97.5%, 85.7%, and 33.3% for 250, 400, and 750 microstrain levels, respectively, when the asphalt binder content is lower than the optimum. Onayev and Swei [16] reported similar findings.

CONCLUSIONS

Based on the conducted testing and limitations of materials, the following observations and recommendations can be made.

1. Four stages of failure could be detected in the asphalt concrete when practicing dynamic flexural stresses regardless of the implemented constant strain levels.

2. High binder content has extended the fatigue life of asphalt concrete to 25% and 16.6% for 250 and 400 microstrain levels, respectively, while low binder content has decline it by 97.5%, 85.7%, and 33.3% for 250, 400, and 750 microstrain levels, respectively, as compared with the mixtures prepared with optimum binder content.
3. The first stage of failure occurs early with sharp trend of decline in the stiffness due to possible materials organization and orientation of solid particles of the asphalt concrete mixture, which provide a seating effect.
4. The second stage of failure shows gentle decline in the stiffness and is associated with micro crack formation and consumes more time up to 20 seconds.
5. The third stage of failure exhibits a sharp trend of decline in the stiffness and is associated with macro crack formation.
6. The fourth stage of failure exhibits almost linear trend of decline in the stiffness and the asphalt concrete consumes more time to creep or fracture based on the binder content.

REFERENCES

1. Abojaradeh M, Witczak M, Mamlouk M, Kaloush K. Validation of initial and failure stiffness definitions in flexure fatigue test for hot mix asphalt. J Testing Eval. 2007; 35 (1): 95–102.
2. Chen A, Airey G, Thom N, Litherland J, Nii-Adjei R. Modelling the stiffness development in asphalt concrete to obtain fatigue failure criteria. Construct Build Mater. 2021; 306 (1): 124837. doi: 10.1016/j.conbuildmat.2021.124837.
3. Bessa I, Vasconcelos K, Branco V, Branco V, Nascimento L, Bernucci L. Prediction of fatigue cracking in flexible and semi-rigid asphalt pavement sections. Int J Pavement Res Technol. 2023; 16: 563–575. doi: 10.1007/s42947-021-00148-5.
4. Abhijith BS, Narayan SPA. Evolution of the modulus of asphalt concrete in four-point beam fatigue tests. ASCE J Mater Civil Eng. 2020; 32 (10): 04020310.. doi: 10.1061/(ASCE)MT.1943-5533.0003354.
5. Mazurek G, Iwański M. Modelling of asphalt concrete stiffness in the linear viscoelastic region. IOP Conf Ser Mater Sci Eng. 2017; 245: 032029. doi: 10.1088/1757-899X/245/3/032029.
6. Sarsam SI. Thermal behavior of asphalt concrete under various microstrain levels. Discovery. 2023; 59: e11d1004.
7. Pradhan N, Henning T, Wilson D. Development of pavement deterioration modeling in New Zealand – a review of achievements. Report DT/2000/182001. HTC Infrastructure Management Ltd; 2000.
8. ASTM International. Road and Paving Materials, Annual Book of ASTM Standards, Volume 04.03, Standard Test Method for Pulse Velocity through Concrete. West Conshohocken, PA, USA: ASTM International; 2015.
9. SCRB. Standards Specification for Roads & Bridges. Baghdad, Iraq: State Commission of Roads and Bridges, Ministry of Housing & Construction; 2003.
10. Sarsam S, Alwan A. Assessing fatigue life of super pave asphalt concrete. Am J Civil Struct Eng. 2014; 1 (4): 88–95.
11. EN 12697–33. Bituminous Mixtures – Test Methods for Hot Mix Asphalt – Part 33: Specimen Prepared by Roller Compactor, 2007. Brussels, Belgium: European Committee for Standardization; 2007.
12. Sarsam SI. Influence of constant strain levels on the viscoelastic properties of asphalt concrete. HBRP J Sustain Construct Eng Project Manage. 2023; 6 (1): 19–27. doi: 10.5281/zenodo.7804196.
13. AASHTO T-321. Method for Determining the Fatigue Life of Compacted Hot-Mix Asphalt (HMA) Subjected to Repeated Flexural Bending, AASHTO Provisional Standards. Washington, DC, USA: AASHTO; 2010.
14. Sarsam S. Assessing asphalt concrete deterioration model from in-service pavement data. TRB Conference, Developing a Research Agenda for Transportation Infrastructure Preservation and Renewal Conference, TRB, Keck Center of the National Academies, Washington, DC, November 12–13, 2009.

15. Sarsam S. Assessment of the deterioration model for asphalt concrete pavement. J Asian Sci Res. 2019; 9 (7): 71–80. doi: 10.18488/journal.2.2019.97.71.80.
16. Onayev A, Swei O. IRI deterioration model for asphalt concrete pavements: capturing performance improvements over time. Construct Build Mater. 2021; 271: 121768. doi: 10.1016/j.conbuildmat. 2020.121768.

